EXPERIMENTAL INVESTIGATION OF JETS PRODUCED BY ROTATING FULLY DEVELOPED PIPE FLOW

Luca Facciolo, Nils Tillmark
KTH Mechanics,
SE-100 44 Stockholm, Sweden
facciolo@mech.kth.se, nt@mech.kth.se

Alessandro Talamelli*
DIEM (Sede di Forlí),
Universitá di Bologna
47100 Forlí, Italy
talamelli@mail.ingfo.unibo.it

ABSTRACT

The flow field of a turbulent jet emerging from a rotating pipe has been experimentally studied for three Reynolds numbers and for different swirl values. The investigation of the mean and fluctuating axial and azimuthal velocity profiles, performed with Laser Doppler Velocimetry, includes the near exit and the transitional jet region. The data, together with the axial decay and turbulence intensity along the centreline, show the large effects of the swirl number on the flow field development. Relatively small effects are observed to be caused by variations in the Reynolds number. The entrainment results are strongly affected by the swirl and by the Reynolds number due to changes in the vortical structures. Spectra, obtained by means of hot wire anemometry, show that the swirl number does not affect the characteristic frequencies measured at the jet axis.

INTRODUCTION

Swirling jets, where an azimuthal velocity is superimposed on the axial flow, are of importance in many technical and industrial applications. For instance, they are used in combustion systems both to enhance the forced convective cooling, to increase turbulent mixing of fuel with air and to stabilize the flame. Despite the importance of this type of flow and the large number of studies carried out in the past, there is still a lack of fundamental experimental data over a wider range of the Reynolds number and swirl number, to enhance the physical understanding of this type of flow as well as to assist in evaluating turbulence models and the development of CFD codes. In fact a large number of previous experimental investigations has used short stationary pipes with blades or vanes at the outlet to attain a swirling jet profile which contains traces of the swirl generator, hence perturbing the axial symmetry of the flow. In order to increase flow homogeneity and to decrease the influence of upstream disturbances, axi-symmetric contractions are used before the jet exit. However, in this way, swirled jets with top-hat exit profiles, characterized by thin mixing layers, are obtained. These type of jets may differ significantly from several industrial applications where fully developed pipe flow may better represent the real boundary conditions. In this paper a preliminary analysis on the flow field generated by a fully developed rotating pipe will be described. This is part of a larger project aimed at the studying of the effects of the impingement of a rotating fully developed jets on a flat plate, positioned relatively close to the pipe exit. For this reason the present experimental study is limited to the analysis of the initial near-exit and intermediate or transitional region.

*also at KTH Mechanics

EXPERIMENTAL APPARATUS AND PROCEDURES

The experiment has been carried out at the fluid physics laboratory of the Royal Institute of Technology (KTH) in Stockholm. The experimental set-up, specifically designed for this purpose, uses air as working fluid, and produces a fully developed turbulent swirling pipe flow without any reminisces of inlet disturbances in the jet. Figure 1 shows a schematic of the apparatus. The swirling pipe flow is produced by a 6 m long (L), axially rotating, steel pipe mounted inside a rigid framework and supported by ball bearings. The pipe is belt-driven by an electric DC motor with feedback circuit to ensure a constant rotation rate up to the maximum 1400 rpm. The inner diameter (D) of the pipe is 60 mm and the inner surface is honed. The outlet of the pipe is at the centre of a stationary rectangular flat aluminium plate (80 cm $\times$ 100 cm) mounted flush with the plate surface. The jet emerges horizontally into ambient still air 1.2 m above the floor and far away from any other physical boundaries. The inlet end of the rotating pipe is connected by a coupling box to the rest of the apparatus. In order to accelerate the swirling motion, a honeycomb is placed inside the rotating pipe immediately downstream of the inlet. The air comes from a centrifugal fan, passes a flow meter (orifice meter with pressure transducer and instrumentation) and is conveyed into a settling chamber to reduce any fluctuations from the upstream flow system. From the settling chamber three pipes run radially into a cylindrical stagnation chamber distributing the air evenly. The flow passes an axial honeycomb to reduce lateral velocity components and to further reduce remaining pressure fluctuations one end of the cylindric settling chamber is covered with an elastic membrane. Finally, the stagnant air leaves the chamber through an axially aligned pipe at the centre of the chamber. The downstream end of the pipe is directly connected to the coupling box and to achieve a symmetric smooth inflow the pipe is provided with an inlet funnel.

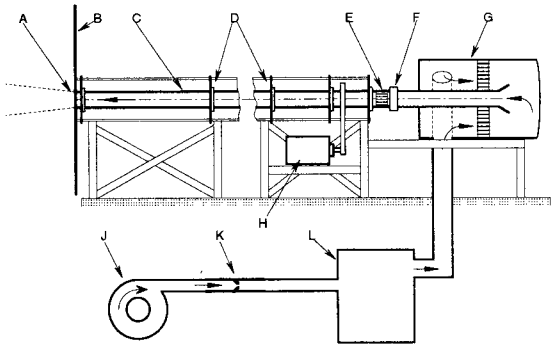

Figure 1: Schematic of the experimental setup. A) Pipe outlet, B) Aluminium plate, C) Rotating pipe. Length 6m, inner diameter 60mm, D) Ball bearings, E) Honeycomb fixed to the pipe, F) Coupling-box between rotating and stationary pipe, G) Stagnation chamber, H) DC- motor, J) Fan, K) Flow meter, L) Settling chamber.

Laser Doppler Velocimetry (LDV) has been used to obtain mean and fluctuating velocity components in both the azimuthal and axial directions. The LDV system is a single component FlowLite system from DANTEC comprising a single velocity component backscatter fiber optics probe with a beam expander, a 310 mm lens and signal analyzer of correlation type. The system is equipped with a Bragg cell providing a frequency shift to be able to distinguish the different flow directions. The probe head is mounted in a rotating holder and the head is rotated 90° along its optical axis to measure the second velocity component. The measuring volume dimensions are: $0.81\times0.09\times0.09$ mm^3 with the largest dimension along the optical axis. Most of the measurements were carried out with the optical axis perpendicular to the pipe axis. Therefore, axial and azimuthal velocities could be directly measured. However, in the close vicinity of the pipe orifice the inclination angle was changed 12° in order to measure both velocity components at the outlet. The data rate varied depending on the measurement position but the sampling was stopped either at 12000 samples or after 240 s. To acquire statistically independent samples the sampling rate was limited to 100 Hz.
The particles used for the LDV measurements are small droplets of condensed smoke of polyethylenglycol. They are injected into the air at the inlet of the centrifugal fan. No stratification of the particles in the outlet jet has been found even at the highest swirl rates. Spectral analysis has been carried out using Hot-Wire anemometry (HW) data obtained by an X-wire probe giving two velocity components simultaneously. A comparison between the two methods was also made and some of the data has also been checked against Pitot-probe and single-wire measurements. The different methods give similar results except in regions with large velocity gradients where the hot-wire data have to be corrected (further discussed in the text below). The X-wire probes are made in the lab and the wire has a diameter of 2.5 μm, is 1.3 mm long and the distance between the wires is 1.5 mm giving a measurement volume of about 1 mm in side length. The probes are calibrated in the potential core of a small laminar air jet in a separate facility operating with air at the same temperature.

To compensate for velocity gradients, the velocity data are processed by means of "a posteriori" correction procedures similar to the one developed by Talamelli et al. (2000) and used to correct hot-wire measurements in the near wall region of a boundary layer. The light source used in the flow visualisations was a 2 W Argon-Ion laser while polyethylenglycol smoke was used as seeding.

X/D :	0 – 10
r/R :	x-axis
S :	0, 0.2, 0.5
$Re\times10^{-3}$:	12, 24, 33.5

Table 1: Velocity measurements along the jet axis

X/D :	0	2	6
$\lvert r/R\rvert$:	≤1	≤ 2	≤2.5
S :	0, 0.2, 0,5	0, 0.2, 0,5	0, 0.2, 0,5
$Re\times10^{-3}$:	12, 24, 33.5	12, 24, 33.5	12, 24, 33.5

Table 2: Velocity measurements at different X/D positions

A cylindrical coordinate system (r,θ,x) is used with the x-axis in the downstream direction along the pipe axis with the origin at the pipe outlet. The mean velocity and rms value for the axial and azimuthal component are U and u', V and v' respectively. The swirl number, S, and Reynolds number, Re, are V_w/U_b and U_bD/ν respectively where $U_b = Q/(\pi D^2/4$, is the mean bulk velocity (Q is the volume flow rate), V_w is the azimuthal velocity at the pipe wall and ν the kinematic viscosity of the fluid. A number of velocity measurements with both HW and LDV was carried out and the different values of the parameters are summarized in table 1 and 2. In the figures a horizontal traverse along the radius from one side of the jet to the other side is denoted using negative and positive values of r.

RESULTS AND DISCUSSION

The pipe outlet conditions are of great importance since they represent the initial conditions for the downstream jet development. The present experimental facility has been designed to generate a fully developed turbulent swirling pipe flow. In figure 2 mean and fluctuating velocity components measured at the pipe exit are shown. The figure shows the effects of varying both Reynolds number and swirl intensity. Due to the symmetry of the profiles only half of them are presented in figure 2. A complete characterisation of the pipe outlet conditions is also of great importance for the validation of CFD codes since they require well defined boundary conditions.

As is shown in figure 2 and 3 both the mean axial and azimuthal velocity profiles seem to be only slightly affected by a change in the Reynolds number. The figures point out the difference between the basic turbulent pipe flow and the swirled flow at the pipe exit. The pipe rotation influences the mean streamwise velocity component such that the maximum velocity in the centre of the pipe increases while the velocity close to the wall decreases. This decrease of the axial component causes a small drop of the wall friction hence decreasing the overall pressure losses of the set-up. Of course, the flow rate was adjusted to keep the Reynolds number constant when the swirl was increased.

On the right side of the figure streamwise turbulent intensity u'/U_b for different swirl and Reynolds numbers are shown. In this case the Reynolds number seems to affect the turbulence intensity, which, for a fixed swirl number, appears to be slightly larger for low Reynolds number. The swirl decreases the turbulence level, especially in a region

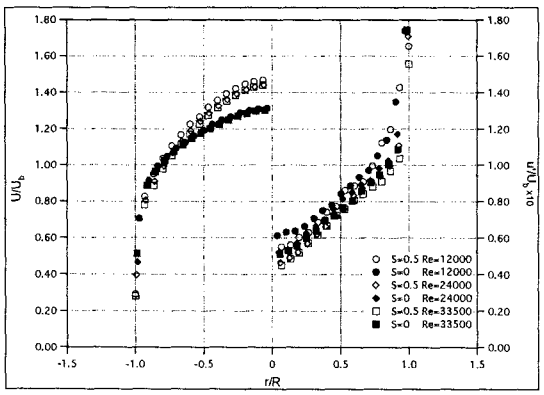

Figure 2: Axial velocity at the pipe outlet S=0, 0.5 (LDV).

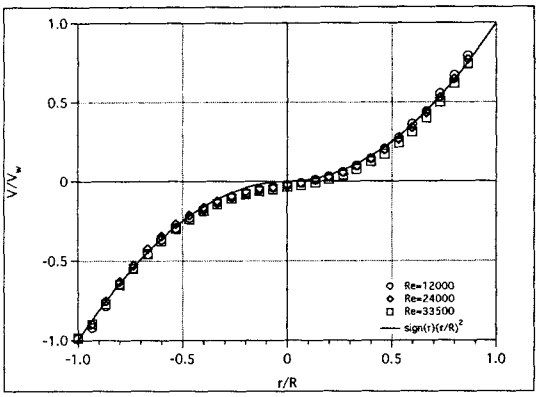

Figure 3: Mean azimuthal velocity. X/D=0, S=0.5 (LDV).

close to the pipe axis. This may be related to the stabilizing effect of the rotation, which can be seen also in the mean velocity profile (see Imao et al., 1996) The fluctuating azimuthal component at the outlet (figure 4) shows a slightly different behaviour. In fact, in this case the reduction due to the swirl seems to be more pronounced approaching the wall, and only very small changes can be seen at the pipe axis.

Looking at figure 3 it can be seen that the mean azimuthal velocity at the pipe exit assumes a shape which is very close to a parabolic distribution. At a first sight, it may be surprising that the mean flow field of a rotating pipe flow deviates from solid body rotation, even though it was already found in previous investigations (see Imao et al., 1996). In a cylidrical coordinate system the equation for the mean azimuthal velocity can be reduced to the following:

$$\nu\left(\frac{d^2V}{dr^2}+\frac{1}{r}\frac{dV}{dr}-\frac{V}{r^2}\right)=\frac{d}{dr}(\overline{vw})+2\frac{\overline{vw}}{r} \qquad (1)$$

This equation can be integrated twice, first from 0 to r, and thereafter from r to R to give (see Wallin & Johansson, 2000)

$$V(r)=V(R)\frac{r}{R}-\frac{r}{\nu}\int_r^R\frac{\overline{vw}}{r}dr \qquad (2)$$

The first term on the right hand side gives the solid body rotation whereas the second term gives a contribution from the Reynolds stress $\overline{vw}$. As was shown in figure 3 the mean azimuthal velocity distribution could be described accurately by the expression $\frac{V(r)}{V(R)}=(\frac{r}{R})^2$for each Reynolds and swirl number investigated, which then can be used to obtain an expression from eq. 2 of $\overline{vw}$ such that

$$\frac{\overline{vw}}{U_b^2}=\frac{2S}{Re}\frac{r}{R} \qquad (3)$$

i.e. the distribution is linear except of course close to the pipe wall. There are both qualitative and quantitative numerical verification of such a behaviour, see Speziale et al. (2000) and Orlandi & Fatica (1997). For the parameter values used, S =0.5 and Re =20000 the maximum value of the RHS is $0.5\cdot10^{-4}$ which corresponds well with the value obtained by Speziale et al. (2000).

Values of the skewness and flatness factors of the streamwise velocity together with the spectra measured at the jet exit (figure 5 show that the flow inside the pipe is close to a fully developed state. All spectra scale when normalised by the bulk velocity and pipe diameter ($St=fD/U_b$).

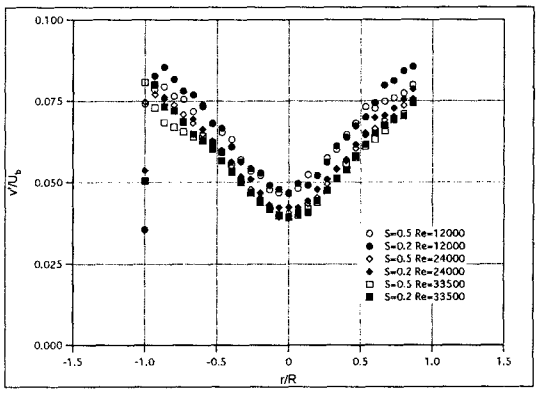

Figure 4: Azimuthal turbulence intensity at X/D=0, S=0.2, 0.5 (LDV).

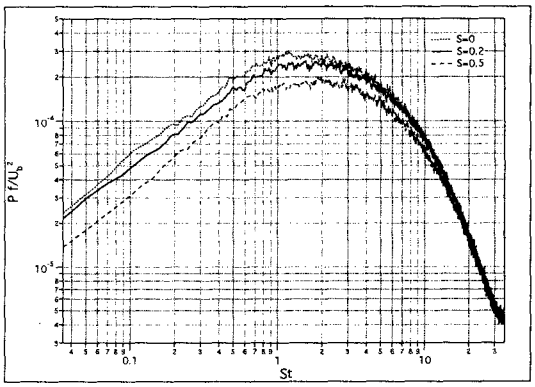

Figure 5: Spectra at outlet centerline Re=33500 (X-HW).

The mean axial velocity along the centreline, U/U_b, its dependence on swirl rate and Reynolds number are shown in figures 6 and 7. The figures display that the axial development of the jet from the pipe outlet to X/D=10 could be separated into two regions, the mixing region and transition region (see Beér & Chigier (1972)). The first region extends from the pipe exit to 3-4 pipe diameters downstream, where the potential core ceases, while the second region covers the incipient part of the developing jet flow. Close to the outlet the velocity decays along the axis is small, approximately linear and the axial velocity increases with swirl rate. The small decline of the axial velocity going downstream is explained by the flattening of the velocity profile in the central part of the core whereas the increase in centreline velocity

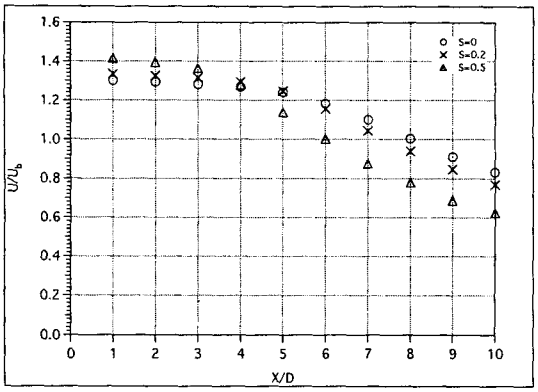

Figure 6: Axial velocity at the center line Re=24000, S=0, 0.2, 0.5 (LDV).

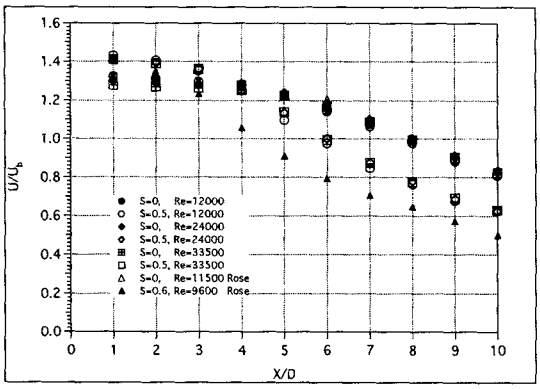

Figure 7: Axial velocity at the center line. Re=12000, 24000, 33500; S=0, 0.5 (LDV).

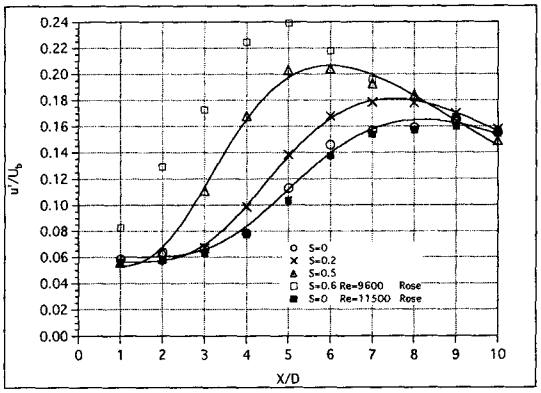

Figure 8: Turbulent intensity at center line, Re=12000 (LDV). (Full lines are trend lines)

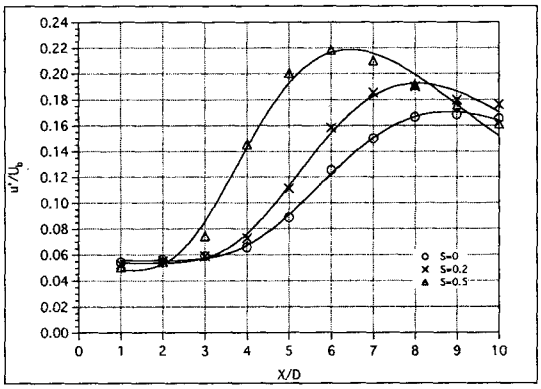

Figure 9: Turbulent intensity at center line, Re=24000 (LDV). (Full lines are trend lines)

is due to the development of a less blunt velocity profile at the outlet with increasing rotation (see figure 12). In the region downstream of the potential core the decline of velocity is substantially larger and increases with swirl rate whereas the variation in slope with Reynolds number is small. Another effect of the swirl seen in the figures is the influence on the form of the velocity decay curve. Without any swirl the decay is almost linear but for increasing swirl the straight line becomes gradually more curved. Included in figure 7 are are also data (Rose (1962)), on a free jet emerging from a stationary and rotating pipe with L/D = 100 at Reynolds numbers similar to presents. The data from the non-rotating cases fall on top of each others while in the rotating case the trend is the same but the fall off is still higher which may be explained by the higher swirl number (0.63).

The turbulence level of the axial component, u'/U_b, along the axis, at the same Reynolds number as in the previous figures, is shown in figure 8 and 9. The turbulence level close to the outlet is only weakly affected by Reynolds number and swirl rate. Downstream the mixing region the turbulence level increases significantly, reaches a maximum and then decreases. The curves have a crossing point at around X/D = 10. The figures show that the onset of the increase in turbulence level moves upstream as the swirl is increased due to the enhanced mixing (with the associated decrease in core length) and that the turbulence maximum moves likewise. However the axial position of the peak is almost constant for each swirl rate irrespectively of the Reynolds number. These trends are supported by the data by Rose (1962) also included in figure 8.

The evolution of the mean axial velocity profile at three downstream positions with and without swirl is shown in figure 12. The graphs clearly show the swirl influence on the U/U_b profile at a fixed Reynolds number of 24000. At short distances downstream of the pipe outlet, $X/D \leq 2$, the axial velocity in the central region of the jet increases for the rotating pipe whereas further downstream at $X/D = 6$, i.e. downstream of the potential core region, the velocity in the central region becomes smaller. At position X/D = 2 and X/D = 6 the mean velocity increases with rotation for $\mid r/R \mid > 1$, i.e. the jet expands in the radial direction. The figure shows that the different profiles have a common crossing point at about $\mid r/R \mid = 1$ and U/U_b=0.6, a characteristic that is also found in the other measurements at Reynolds number Re=12000 and Re=33500 and at S=0.2.

By integrating the velocity profiles it is possible to estimate the air entrainment of the different configurations. A non-linear least square fitting procedure is used in order to extrapolate the mean velocity profiles in the external part of the mixing layer. Due to the limited number of streamwise measurement positions the flow rate values are reported in Table 3. In the table the flow rate normalized by its value at the pipe outlet is shown. The accuracy of the above measurement was assessed by checking that the overall amount of flow momentum remains constant moving downstream.

Table 3 shows that an increase of the flow rate is observed by moving downstream for all the configurations analysed.

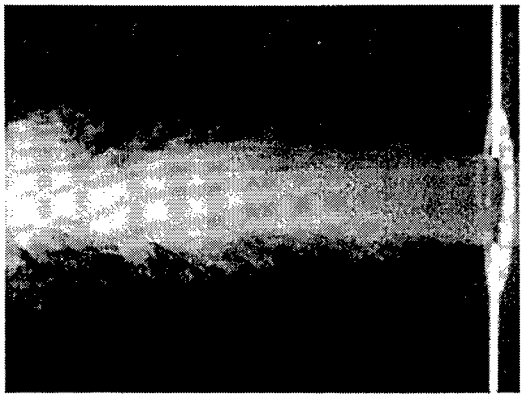

Figure 10: Instantaneous flow visualization Re=12000,S=0

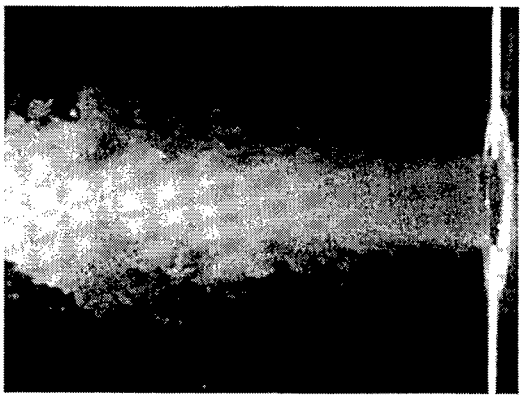

Figure 11: Instantaneous flow visualization Re=12000, S=0.5

	X/D	S=0	S=0.2	S=0.5
Re=12000	2	1.52	1.61	2.01
	6	2.52	2.77	3.16
Re=24000	2	1.39	1.45	1.52
	6	2.14	2.33	2.80
Re=33500	2	1.36	1.41	1.50
	6	2.18	2.25	2.60

Table 3: Entrainment: Q/Q_0

This is of course due to the engulfment of ambient fluid by the vortical structures present in the mixing layer and generated by a Kelvin-Helmoltz instability mechanism at the pipe exit. The swirl increases significantly both the entrainment and the jet spreading. This is also confirmed by the flow visualizations shown in figure 10 and 11. This increase in entrainment due to the pipe rotation seems to be reduced by increasing the Reynolds number. The reason for this Reynolds number dependence is not clear. By looking at the flow visualizations it may be concluded that it is an effect related to the more pronounced eddy structures formed in the mixing layer, which may enhance the entrainment of fluid from the environment.

In order to get some information concerning the vortical structures generated at the pipe exit, a spectral analysis of both the axial and azimuthal velocities obtained from cross-wire measurements was carried out. Figure 16 shows that at X/D=2 a distinct peak in the u-components is formed. If the frequency is normalized by the bulk velocity and pipe diameter, a Strouhal number of about 0.5 is obtained, which remains constant for all swirl numbers studied here. This peak is also present at the other Reynolds number studied.

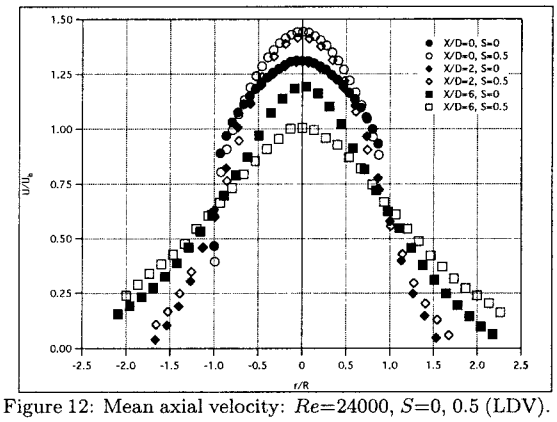

Figure 12: Mean axial velocity: Re=24000, S=0, 0.5 (LDV).

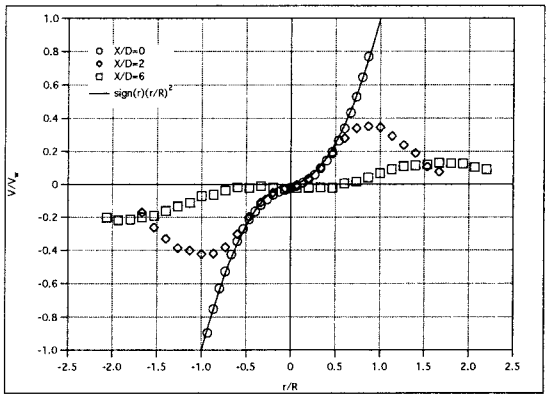

Figure 13: Mean azimuthal velocity. Re=24000, S=0.5 (LDV).

This behaviour shows that the rotation (at least for the values analysed) does not affect the instability mechanism of the jet-column mode even though a value of 0.5 is slightly larger than the ones obtained downstream of a single axisymmetric jet. Further dowstream the peak starts to broaden due to the development and breakdown of the structures, however the frequency seems to remain the same.

Figure 13 shows the downstream evolution of the normalized mean azimuthal velocity V/V_w profiles. As stated above, at the pipe outlet, the velocity profile closely follows a profile proportional to r^2/R^2). The figure shows that further downstream the radius of the potential core decreases but the "parabolic" nature of the azimuthal velocity seems to persist in the central region as long as the jet is not fully developed.

The influence on turbulence by rotation is shown in figure 14. The streamwise turbulence intensity u'/U_b, is compared for a jet with and without swirl at one Reynolds number (24000) and at three different downstream positions X/D=0, 2 and 6. Only small changes are observed at the pipe outlet. Further downstream the turbulence intensity u'/U_b increases at off-axis positions between 20% and 40%. At X/D=2 the largest changes are at r/R=0.5 for the rotating pipe. Large changes are also found in the outmost part of the jet but at a much lower absolute level. At X/D=6 the main difference between the swirling and non-swirling jet is found around the centreline where the turbulence level is almost doubled as the swirl number S goes from 0 to 0.5 an effect already seen in figure 9 and discussed in that context.

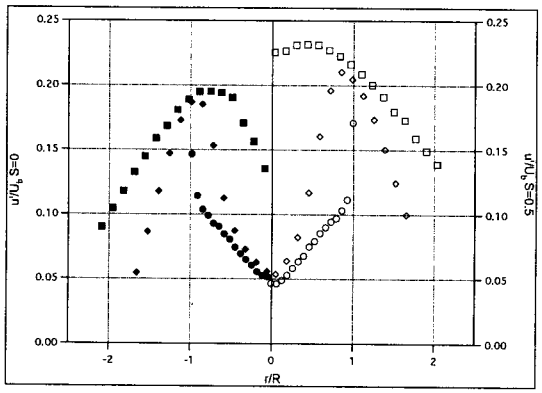

Figure 14: Radial turbulence intensity at Re=24000, S=0 and S=0.5 (LDV), see fig 12 for symbols.

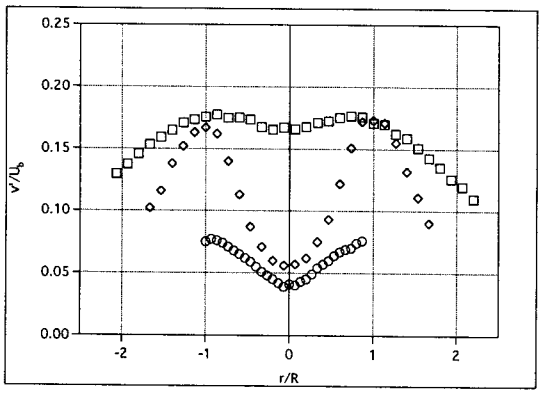

Figure 15: Azimuthal turbulence intensity at Re=24000, S=0.5 (LDV), see fig 12 for symbols.

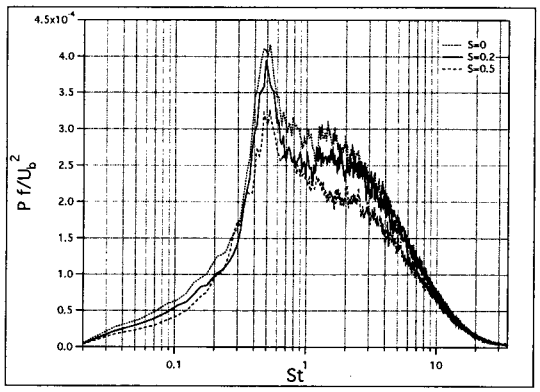

Figure 16: Spectra at centerline X/D=2 Re=33500 (X-HW).

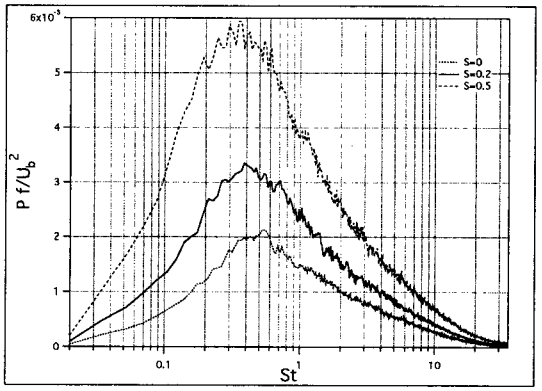

Figure 17: Spectra at centerline X/D=6 Re=33500 (X-HW).

CONCLUSIONS

In this paper an experimental analysis of the flow field produced by a fully developed turbulent rotating pipe flow is presented. In order to achieve well controlled, symmetric and homogeneous initial conditions of the flow, great care was taken in the design and set-up procedures of the experimental apparatus. The initial conditions have been thoroughly analysed and confirm that the flow is fully developed. The experiments show that the swirl number, even if relatively small, has large effects on both mean and fluctuating components. The mean azimuthal velocity profiles show a parabolic behaviour in accordance with previous experiments and simulations. This tendency allows the $\overline{vw}$ distribution along the pipe radius to be estimated. The Reynolds number does not alter significantly the mean component distributions, and only small changes are observed in the turbulence intensities.

The swirl number has a large effect on the flow development. An increase in both spreading and entrainment rate has been observed. Moreover the Reynolds number seems to affect the flow field after the pipe exit. Flow visualizations show a more regular behaviour of the vortical structures generated at the jet exit when the velocity inside the pipe is decreased. This tendency may explain the increase in the mass flow entrainment observed at low Reynolds number. Spectral analysis shows that the rotation, at least for the values analysed in this paper, does not affect the frequencies related to the jet column mode.

This research has been sponsored by the Swedish Energy Agency (STEM). The support is greatefully acknowledged.

REFERENCES

Beér, J.M. & Chigier, N.A., 1972, *Combustion aerodynamics*, Applied Science Publishers LTD, London.

Eggels, J.G.M., Unger, F., Weiss, M.H., Westerweel, J., Adrian, R.J., Friedrich, R. & Nieuwstadt, F.T.M., 1994, "Fully developed turbulent pipe flow: a comparison between direct numerical simulation and experiment", *J. Fluid Mech.*, Vol. 268, pp. 175-209.

Imao, S., Itoh, H. & Harada, T., 1996, "Turbulent characteristics of the flow in an axially rotating pipe", *Int. J. Heat and Fluid Flow*, Vol. 17, pp. 444-451.

Orlandi, P. & Fatica, M., 1997, "Direct simulations of turbulent flow in a pipe rotating about its axis", *J. Fluid Mech.*, Vol. 343, pp. 43-72.

Pratte, B. D. & Keffer, J.F., 1972,"The swirling turbulent jet", *J. Basic Eng.*, Vol. 94, pp. 739-748.

Rose, W. G., 1962, " A Swirling Round Turbulent Jet", *J. Appl. Mech.*, Vol. 29, pp. 615-625.

Speziale, C.G., Younis, B.A, & Berger, S.A., 2000, "Analysis and modeling of turbulent flow in an axially rotating pipe", *J. Fluid Mech.*, Vol. 407, pp. 1-26.

Talamelli, A., Westin, K. J. A. & Alfredsson, P. H., "An experimental investigation of the response of hot wire X-probes in shear flows", *Exp. Fluids*, Vol. 28, pp. 425-435.

Wallin, S. & Johansson, A.V., 2000,"An explicit Reynolds stress model for incompressible and compressible turbulent flows", *J. Fluid Mech.*, Vol. 403, pp. 89-132.